Activation mechanism of methane-derived coke (CH_x) by CO_2 during dry reforming of methane – comparison for Pt/Al_2O_3 and Pt/ZrO_2

Katsutoshi Nagaoka [a], Kulathuiyer Seshan [b], Johannes A. Lercher [c] and Ken-ichi Aika [a,*]

[a] *Department of Environmental Chemistry and Engineering, Interdisciplinary Graduate School of Science & Engineering, Tokyo Institute of Technology, 4259 Nagatsuta, Midori-ku Yokohama 226-8502, Japan*
E-mail: kenaika@chemenv.titech.ac.jp
[b] *University of Twente, Faculty of Chemical Technology, PO Box 217, 7500 AE Enschede, The Netherlands*
[c] *Technical University of Munich, Department of Physical Chemistry, D-85748 Garching, Germany*

Received 2 August 2000; accepted 21 September 2000

The reaction of methane-derived coke (CH_x: intermediate of the reforming reaction and also a source of coke deposition) with CO_2 was studied on supported Pt catalysts in relation with CO_2 reforming of methane. Temperature-programmed hydrogenation (TPH) was performed to investigate the reactivity of coke deposition after the catalyst was exposed to CH_4/He at 1070 K. Coke on Pt/Al_2O_3 could be hydrogenated around 873 K, while for Pt/ZrO_2 this was above 1073 K. The results indicate that the reactivity of coke with hydrogen was higher on Pt/Al_2O_3 than on Pt/ZrO_2, which was different from the reactivity of coke towards CO_2. Thus, the reactivity of CO_2 was studied and compared on these catalysts by several technics. The amount of CO evolution was measured during CO_2 flow at 1070 and 875 K. Rate and amount of converted CO_2 were higher on Pt/ZrO_2 than on Pt/Al_2O_3. Pt/ZrO_2 was proven to react with CO_2 to produce CO and active oxygen ($CO_2 \rightarrow CO + O$) (probably on its oxygen defect site) more easily than Pt/Al_2O_3.

Keywords: CH_4/CO_2 reforming, supported Pt catalysts, reactivity of coke with CO_2, reactivity of coke itself, reactivity of CO_2, oxygen defect site

1. Introduction

CO_2 reforming of methane is attractive for generating synthesis gas with H_2/CO ratio of unity, suitable for synthesizing formaldehyde, oxoalcohols, and polycarbonates. Furthermore commercial interest lies in combining CO_2 reforming with steam reforming and generating syngas with different H_2/CO ratios in the range of 1/1 to 3/1 [1]. Supported nickel or platinum catalysts have been studied as catalysts for the CO_2 reforming of methane [1–12]. Catalyst deactivation is a serious problem for this reaction, which is at least partly inflicted by the thermodynamic equilibrium and must be overcome by developing an effective catalyst. There are two causes for catalyst deactivation, i.e., coke deposition [1–12] and sintering of the metal particles [2,3,7,9]. Most authors agree that coke formation is the main cause of the deactivation. Coke originates mainly from two reactions, methane decomposition ($CH_4 \rightarrow C + 2H_2$) and carbon monoxide disproportionation ($2CO \rightarrow C + CO_2$). The former is an endothermic reaction and favored at higher temperatures and lower pressures. On the other hand, the latter is exothermic and favored at lower temperatures and higher pressures.

Pt/ZrO_2 has been found to be stable at a wide temperature range, while Pt/Al_2O_3 and Pt/TiO_2 deactivated under the same conditions [13–16]. We have proposed that the reaction proceeds mainly at the interface between Pt and the support at lower temperatures, but takes place either on the interface and on Pt particles at higher temperatures ($\geqslant$1070 K) [16]. The reaction involves activation of methane on Pt particles to yield molecular hydrogen and partially dehydrogenated methane (CH_x) as the surface species. This CH_x species is oxidized by activated CO_2. As many researchers have concluded [2–11], the cause of deactivation over Pt/Al_2O_3 was due to coke deposition on the catalytic reactive sites and not due to sintering of Pt particles. At a relatively high temperature (1070 K), a part of CH_x species derived from CH_4 remains on the catalyst without being oxidized by CO_2 and gradually covers the active sites. After a while only the perimeter of Pt particles remains as the active site. The coke deposition is brought about by an imbalance between CH_4 decomposition on Pt particles and its oxidation by activated CO_2. On the other hand, coke hardly deposits on Pt/ZrO_2 and the catalyst keeps the stable activity for long periods of time. A combination of three factors is concluded to balance the two steps on Pt/ZrO_2 in CH_4/CO_2 reforming conditions [1,13–17]: (i) coke on Pt supported on ZrO_2 is more reactive towards CO_2 than coke on Pt supported on Al_2O_3; (ii) CH_4 decomposition is slower on Pt/ZrO_2 than on Pt/Al_2O_3; (iii) coke which may cover active sites is hardly formed on ZrO_2.

The second and third reasons have been discussed in detail in the preceding paper [16]. However, it is still not

---

[*] To whom correspondence should be addressed.

clear why coke on Pt supported on ZrO_2 is more reactive towards CO_2 than coke on Pt supported on Al_2O_3. As the reactants are methane-derived coke (CH_x) and CO_2, the reactivity of those species would bring about the difference in reactivity of coke with CO_2. In this communication, we focus on the reactivity of coke and CO_2 on supported Pt catalysts (Pt/Al_2O_3 and Pt/ZrO_2) and its relation to coke deposition at the temperature used for commercial operation (1070 K). Further, the role of support affecting CO_2 reactivity is discussed. Temperature-programmed hydrogenation (TPH) and subsequent temperature-programmed oxidation (TPO) are performed to investigate the reactivity of coke species on supported Pt catalysts which were exposed to CH_4/He (methane as the source of coking). The results are compared with those of temperature-programmed reaction (TPRn) with CO_2 (reproduced from [16]). Further, the amount of CO evolution was measured during CO_2 flow to compare the activation of CO_2 over the supported Pt catalysts and over the sole supports. IR experiments were also carried out to understand the nature of CO_2 adsorption on these catalysts.

2. Methods

2.1. Catalysts preparation

Pt/ZrO_2 and Pt/Al_2O_3 were prepared by the wet impregnation technique. For this purpose, a solution of $H_2PtCl_6 \cdot 6H_2O$ in water (0.01 g-Pt ml^{-1}), ZrO_2 (RC-100, Gimex, Japan), and Al_2O_3 (000–3AQ, AKZO, The Netherlands) were used. The ZrO_2 powder was pressed at 4000 bar for 5 min, while Al_2O_3 was obtained by extruding the gel. The pellets were crushed and sieved to particles with diameters between 0.3 and 0.6 mm. The grains were calcined for 15 h at 1125 K (heating rate 3 K min^{-1}) in flowing air (30 ml min^{-1}) and subsequently impregnated with Pt (0.5 wt%). The catalysts were dried at 365 K for 2 h in a rotating evaporator followed by drying overnight at 395 K in static air. The impregnated grains were calcined for 15 h at 925 K (heating rate 3 K min^{-1}) in flowing air (30 ml min^{-1}). The Pt content of the catalysts was determined by atomic absorption spectroscopy.

2.2. Temperature-programmed hydrogenation (TPH), temperature-programmed oxidation (TPO), and temperature-programmed reaction (TPRn) with CO_2

TPH, TPO, and TPRn with CO_2, were performed in an Altamira AMI-2000 apparatus. 100 mg of catalysts were loaded into a tubular quartz reactor and a thermocouple was placed at the top of the catalyst bed to measure the temperature of the catalyst. The furnace temperature was controlled by an Eurotherm temperature controller. After the catalyst was reduced *in situ* with H_2 for 1 h at 1120 K, the temperature was lowered to 1070 K in He stream and feed gas mixture (CH_4/He (1/1) with a total flow of 28 ml min^{-1}) was introduced to the reactor for the required time. Then the catalyst was kept in He for 30 min at the temperature and the reactor was cooled to 340 K.

For the TPH experiment, the sample was then exposed to a flow of H_2/He (10/90 with a total flow of 30 ml min^{-1}) at 340 K and subsequently heated up to 1273 K (heating rate 10 K min^{-1}). CH_4 ($m/e = 16$), H_2O ($m/e = 18$), CO ($m/e = 28$), and CO_2 ($m/e = 44$) signals were measured with a mass spectrometer. For TPRn with CO_2 and TPO measurements, H_2/He in the above experiment was replaced with CO_2/He (10/90 with a total flow of 30 ml min^{-1}) or O_2/He (5/95 with a total flow of 30 ml min^{-1}), respectively. The final dwell time at 1273 K was 10 min.

2.3. CO evolution measurement during CO_2 flow

200 mg of sample (Pt/ZrO_2, Pt/Al_2O_3, ZrO_2, and Al_2O_3) were loaded into a tubular quartz reactor and a thermocouple was placed at the top of the catalyst layer. The sample was reduced with H_2 for 1 h at 1120 K. After reduction, the temperature of the sample was adjusted to the reaction temperatures (1070 and 875 K) under flowing He. The sample was purged by He to remove residual H_2 for 1 h and CO_2/He (3/1 with a total flow of 40 ml min^{-1}) was fed to the reactor for 30 min (1st run). In these experiments, after the reaction, the catalyst was treated in H_2 and subsequent He at the reaction temperature of the 1st run and CO_2/He (3/1) was fed again to the reactor for 30 min at the temperature (2nd run). The amount of CO evolution was analyzed by a gas chromatograph (Aera M200) equipped with a 2m-MS-5A column and a TCD.

2.4. IR spectroscopic measurement of CO_2 adsorption

The catalyst powder was pressed into a self-supporting wafer. This wafer was placed into a quartz IR cell equipped with KBr windows and was analyzed *in situ* during the reaction by means of transmission absorption IR spectroscopy using a JASCO FT/IR-620 spectrometer (resolution 4 cm^{-1}). After the catalyst was reduced with H_2 at 1073 K for 1 h, the temperature was lowered to 300 K under He flow and a background spectrum was recorded at the temperature. After the catalyst was treated with flowing CO_2 (30 ml min^{-1}) for 30 min and subsequent He (30 ml min^{-1}) for 30 min at 300 K, its IR spectrum was recorded again in He flow.

3. Results

3.1. Temperature-programmed hydrogenation

TPH profiles of $m/e = 16$, 18, 28, and 44 over Pt/Al_2O_3 after exposure to CH_4/He for 10 min are shown in figure 1. We discuss here the contribution of O ($m/e = 16$) fragmentation from H_2O ($m/e = 18$), CO ($m/e = 28$), and CO_2 ($m/e = 44$) to CH_4. The peak intensities of H_2O decreased with temperature, and those of CO and CO_2 were

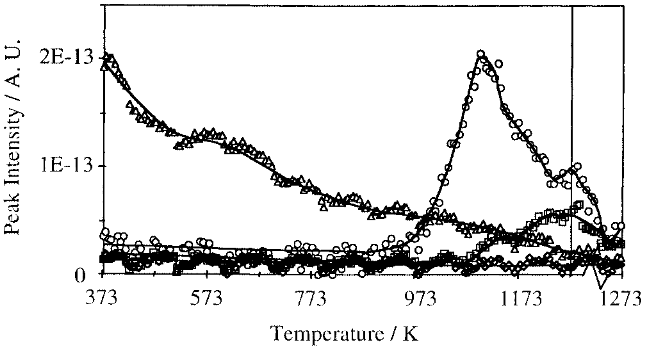

Figure 1. Temperature-programmed hydrogenation (TPH) profiles of m/e = (○) 16, (△) 18, (□) 28, and (◇) 44 for Pt/Al$_2$O$_3$ catalyst after exposure to CH$_4$/He at 1070 K for 10 min.

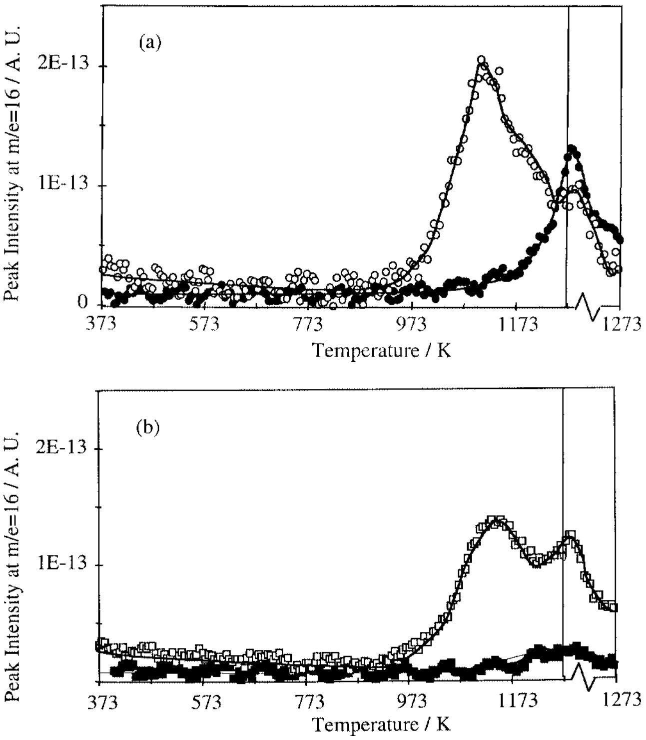

Figure 2. Temperature-programmed hydrogenation (TPH) profiles of $m/e = 16$ for Pt/Al$_2$O$_3$ and Pt/ZrO$_2$ catalysts after exposure to CH$_4$/He at 1070 K for (a) 10 and (b) 60 min. (○) Pt/Al$_2$O$_3$ for 10 min, (●) Pt/ZrO$_2$ for 10 min, (□) Pt/Al$_2$O$_3$ for 60 min, and (■) Pt/ZrO$_2$ for 60 min.

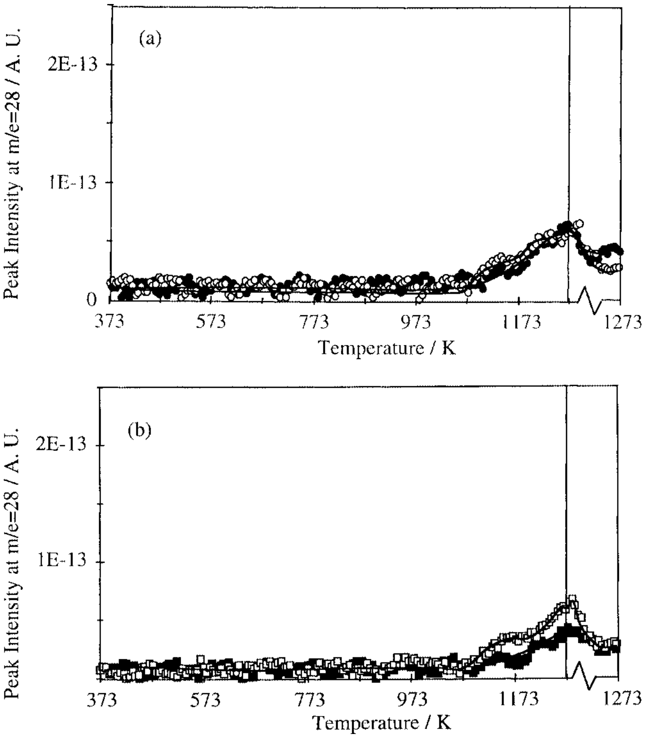

Figure 3. Temperature-programmed hydrogenation (TPH) profiles of $m/e = 28$ for Pt/Al$_2$O$_3$ and Pt/ZrO$_2$ catalysts after exposure to CH$_4$/He at 1070 K for (a) 10 and (b) 60 min. (○) Pt/Al$_2$O$_3$ for 10 min, (●) Pt/ZrO$_2$ for 10 min, (□) Pt/Al$_2$O$_3$ for 60 min, and (■) Pt/ZrO$_2$ for 60 min.

rather smaller than those of $m/e = 16$, indicating the contribution is quite small. Therefore, we ignore these contributions hereafter.

TPH showed increase of peak intensity at $m/e = 16$ and 28, indicating coke was removed from the catalyst as CH$_4$ ($m/e = 16$) and CO ($m/e = 28$). TPH profiles for Pt/Al$_2$O$_3$ and Pt/ZrO$_2$ after exposure to CH$_4$/He (facile coke formation) for 10 and 60 min are shown in figure 2 ($m/e = 16$) and figure 3 ($m/e = 28$). Peaks of CH$_4$ ($m/e = 16$) were observed above 873 K for Pt/Al$_2$O$_3$ after different exposure times, while only a single peak was visible above 1073 K on Pt/ZrO$_2$ even after different exposure times. The results indicate some of the coke on Pt/Al$_2$O$_3$ is more reactive with H$_2$ than that on Pt/ZrO$_2$. For both catalysts, the peaks after exposure to methane for 10 min were larger than those after exposure for 60 min. As the amount of coke would be expected to increase with exposure time, the results imply part of the coke (probably polymerized and stabilized) was not removed from the catalysts by reaction with hydrogen up to 1273 K. On the other hand, the amount and starting temperature (above 1070 K) of CO ($m/e = 28$) formation were almost the same for both catalysts after different exposure times. Coke may have reacted with oxygen (lattice oxygen and/or hydroxyl) on the support above reaction temperature (1070 K).

3.2. Temperature-programmed oxidation following to temperature-programmed hydrogenation

As was discussed in section 3.1, there was a possibility that coke remained on the catalysts after TPH. After TPH (the catalysts were exposed to CH$_4$/He for 10 and 60 min before TPH), TPO was subsequently carried out for supported Pt catalysts, and the profiles of CO$_2$ are shown in figure 4 (catalysts were coked for 10 min) and 5 (catalysts were coked for 60 min). For comparison, in figure 4 TPO profiles without TPH are also shown for catalysts after exposure to CH$_4$/He for 10 min. In these experiments, the peak intensities of CO were in agreement with the fragmentation of $m/e = 28$ from CO$_2$, indicating that coke on the catalyst was converted to CO$_2$ during TPO (not to CO). In TPO profiles (without TPH), a single peak for Pt/ZrO$_2$

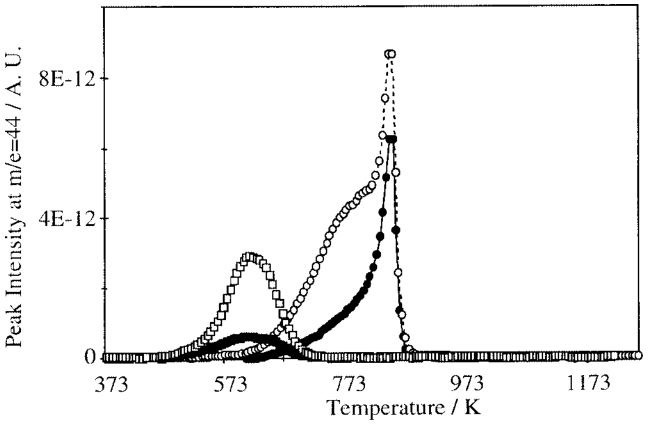

Figure 4. Temperature-programmed oxidation (TPO) profiles over Pt/Al_2O_3 and Pt/ZrO_2 catalysts coked and after TPH (catalysts were treated in CH_4/He at 1070 K for 10 min). (●) Pt/Al_2O_3 after TPH, (○) Pt/Al_2O_3 coked, (■) Pt/ZrO_2 after TPH, and (□) Pt/ZrO_2 coked.

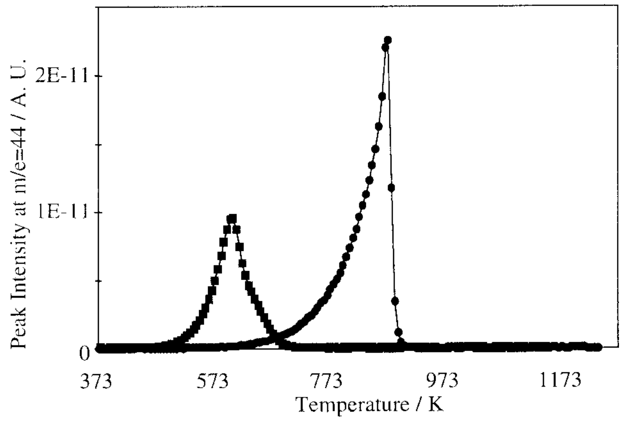

Figure 5. Temperature-programmed oxidation (TPO) profiles for (●) Pt/Al_2O_3 and (■) Pt/ZrO_2 catalysts after TPH (catalysts were treated in CH_4/He at 1070 K for 60 min).

was assigned to coke on Pt particles, and low and high temperature peaks for Pt/Al_2O_3 were assigned to coke on Pt particles and on the support, respectively, in an earlier work [16]. Peaks were observed in the TPO profile (after TPH) for all samples, indicating some coke on Pt (supported on ZrO_2 and Al_2O_3) and most of the coke on the support (Al_2O_3) cannot be removed by reaction with hydrogen up to 1273 K. The results show coke is more easily removed from metallic Pt (which can catalyze hydrogenation) than from Al_2O_3 in the case of Pt/Al_2O_3. As can be expected, the size of peaks (after TPH) after exposure to CH_4/He for 60 min (figure 5) was larger than that (without TPH) after exposure for 10 min (figure 4) for both catalysts, indicating the amount of coke increased with exposure time.

3.3. Temperature-programmed reaction with CO_2

Figure 6 shows the TPRn profiles with CO_2 for Pt/Al_2O_3 and Pt/ZrO_2 after exposure to CH_4/He for 10 min. The results are reproduced from our earlier work [16]. During the experiments, coke was converted to CO (in all experiments contribution of the CO_2 fragment to CO ($m/e = 28$) was subtracted). Our results have indicated that CO is not evolved during experiments with the freshly reduced catalysts (not shown). This rules out the possibility of any significant contribution of the CO_2 dissociation ($CO_2 \rightarrow CO + O$) during TPRn with CO_2. For Pt/Al_2O_3, peaks were observed below and above reaction temperature (1070 K) and these were assigned to coke on Pt and Al_2O_3, respectively. On the other hand, for Pt/ZrO_2 two peaks appeared below reaction temperature and these were assigned to coke on Pt (supported on ZrO_2). We have proved only the coke corresponding to the low temperature peak forms on Pt/ZrO_2 in the presence of a CH_4/CO_2 mixture by changing the exposure time for CH_4/He. Therefore, we have concluded coke on Pt is more easily removed by activated CO_2 on Pt/ZrO_2 than on Pt/Al_2O_3 [16].

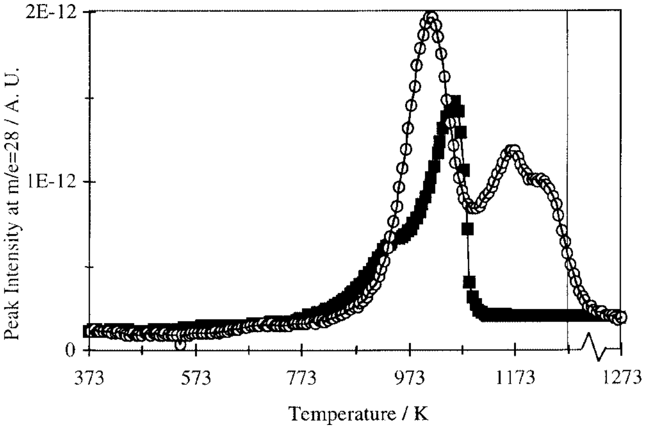

Figure 6. Temperature-programmed reaction (TPRn) with CO_2 profiles for (○) Pt/Al_2O_3 and (■) Pt/ZrO_2 catalysts after exposure to CH_4/He at 1070 K for 10 min.

3.4. CO evolution measurement during CO_2 flow

Time on stream of CO yield on Pt/Al_2O_3 and Pt/ZrO_2 (reduced at 1120 K) during CO_2 flow at 1070 and 875 K was measured, and the results are shown in figure 7. CO_2 flowing over freshly reduced catalysts yields only CO ($CO_2 \rightarrow CO + O$) in the gas phase, and the CO yield decreased with time of exposure. The results are in accordance with an earlier work for Pt/ZrO_2 by CO_2 pulsing at 875 K and IR spectroscopic experiments at 775 K [14]. The decrease of CO yield with time of exposure was explained by blocking of the sites that decompose CO_2 into adsorbed oxygen (O) and CO. In this context, the nature of the adsorbed oxygen still needs to be addressed. The results of EXAFS for Pt/ZrO_2 did not give evidence for the presence of adsorbed oxygen or (surface) oxides of Pt–O, so it is not likely that the oxygen is located on Pt. This is also supported by XANES. Thus, we have concluded that the oxygen is consumed at the metal–support interface [14,17]. In addition, as an earlier work has shown, CO_2 pretreatment increases the conversion of CH_4 (pulsed on Pt/ZrO_2) as compared with H_2 pretreatment; it is likely that adsorbed

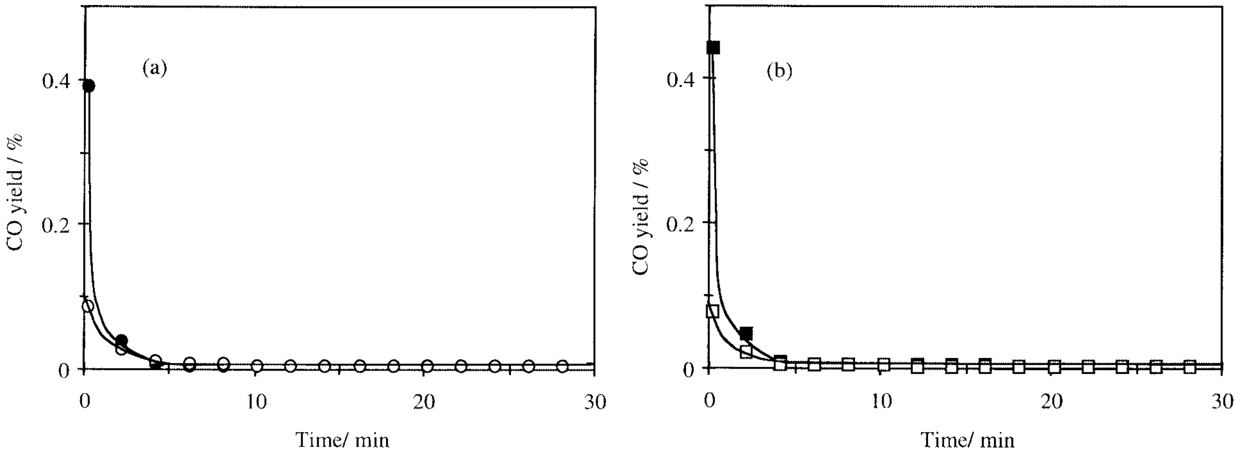

Figure 7. CO evolution for Pt/Al_2O_3 and Pt/ZrO_2 catalysts (reduced at 1120 K) during CO_2 exposure at (a) 1070 K and (b) 875 K. (○) Pt/Al_2O_3 at 1070 K, (●) Pt/ZrO_2 at 1070 K, (□) Pt/Al_2O_3 at 875 K, and (■) Pt/ZrO_2 at 875 K.

Table 1
CO evolution over catalysts during CO_2 exposure at 1070 K.

Catalyst	Run	Temperature (K)		Measured value		Calculated value	
		Reduction[a]	Exposure[b]	(CO evolution (10^{-3}%))		CO_2 conversion (10^{-3}%)	N[c]
				0.2 min	2.2 min	0 min	(10^{-6} mol g-cat^{-1})
Pt/ZrO_2	1st	1120	1070	390	38	473	9.1
	2nd	1070	1070	184	26	216	4.9
Pt/Al_2O_3	1st	1120	1070	87	27	96	3.7
	2nd	1070	1070	78	21	87	3.0
ZrO_2	1st	1120	1070	180	28	210	5.1
	2nd	1070	1070	19	trace (<10)	–	–
Al_2O_3	1st	1120	1070	16	trace	–	–
	2nd	1070	1070	10	trace	–	–

[a] Catalyst was reduced with H_2.
[b] Catalyst was exposed to CO_2.
[c] Number of CO_2 activation site.

Table 2
CO evolution over catalysts during CO_2 exposure at 875 K.

Catalyst	Run	Temperature (K)		Measured value		Calculated value	
		Reduction[a]	Exposure[b]	(CO evolution (10^{-3}%))		CO_2 conversion (10^{-3}%)	N[c]
				0.2 min	2.2 min	0 min	(10^{-6} mol g-cat^{-1})
Pt/ZrO_2	1st	1120	875	440	46	531	10.5
	2nd	875	875	74	20	83	2.8
Pt/Al_2O_3	1st	1120	875	77	20	85	3.0
	2nd	875	875	52	19	57	2.5
ZrO_2	1st	1120	875	11	trace (<10)	–	–
	2nd	875	875	trace	trace	–	
Al_2O_3	1st	1120	875	trace	trace	–	–
	2nd	875	875	trace	trace	–	–

[a] Catalyst was reduced with H_2.
[b] Catalyst was exposed to CO_2.
[c] Number of CO_2 activation site.

oxygen left on the catalyst reacts with methane-derived coke (CH_x) under CH_4/CO_2 condition [14]. The figure showed that the CO yield at 0.2 min was much higher for Pt/ZrO_2 than for Pt/Al_2O_3 at both temperatures, indicating the rate for producing active oxygen is higher on Pt/ZrO_2 than on Pt/Al_2O_3.

The measured CO yield during CO_2 flow over catalysts is compiled in tables 1 (catalyst was reduced with H_2 at

1120 K and exposed to CO_2 at 1070 K in the 1st run, corresponding to figure 7(a)) and 2 (catalyst was reduced with H_2 at 1120 K and exposed to CO_2 at 875 K in the 1st run, corresponding to figure 7(b)). As stated in the first part of the results, before temperature-programmed operations, the catalysts were reduced with H_2 at 1120 K and subsequently exposed to CH_4 at 1070 K (figures 1–6), and more coke was removed by CO_2 on Pt/ZrO_2 than on Pt/Al_2O_3 around 873 K (figure 6). The treatment temperatures in tables 1 and 2 were thus selected.

Since CO_2 reactivity seems to be decreased gradually (figure 7), an exponential time dependency (e^{-kt}) of CO_2 conversion was assumed,

$$CO_2 \text{ conversion } (\%) = \text{CO yield } (\%) = C_0 e^{-kt},$$

where k denotes the rate constant and t time (min).

Now, CO_2 conversion at time 0 (C_0) and the total number of CO_2 converted (N) were calculated and are also shown in tables 1 and 2. N is considered to be the number of active oxygen which reacts with methane-derived coke (CH_x) if it would be supplied.

During the experiments, after the 1st run, the catalyst was reduced again with H_2, purged with He, and subsequently exposed to CO_2 (2nd run) at the same temperature as the 1st run. If we gave the same condition as those of the 1st run (H_2 reduction at 1120 K, He purge, and subsequent CO_2 flow) after the 2nd run, we obtained the same CO concentration as that of the 1st run (3rd run, reproducibility check). The decrease of CO evolution at the 2nd run compared with the 1st run may be due to the decrease of sites accepting O from CO_2. High-temperature treatment with H_2 gives the catalyst more accepting sites of O from CO_2 than low-temperature treatment. Since the temperature of the 2nd run is the same as that for the CH_4/CO_2 reaction condition, the calculated values such as C_0 and N for the 2nd run in tables 1 and 2 must be more practical than for the 1st run. In all conditions, Pt/ZrO_2 had higher performance (C_0 and N: number of active oxygen sites) than Pt/Al_2O_3, indicating the rate of CO_2 activation and the number of active oxygen produced are higher on Pt/ZrO_2 than on Pt/Al_2O_3.

It is noted that oxide itself reacts with CO_2 if it is treated at high temperature. The number of active oxygen produced on ZrO_2 was much higher than that on Al_2O_3 (table 1). So called strong metal–support interaction (SMSI) theory [18] needs Pt on reducible oxide supports, but here the temperature may be high enough to reduce support oxide partly. These results imply the support itself can supply CO_2 activation sites; of course Pt enhances those activities greatly.

3.5. IR spectra of CO_2 adsorption

The adsorption of CO_2 on Pt/Al_2O_3 and Pt/ZrO_2 was investigated by IR spectroscopy at 300 K in order to distinguish the type of carbonates on these catalysts, and the results are shown in figure 8. The bands appeared more clearly at this temperature than the bands that were measured at 775 K by our group [13–15]. Three main bands appeared at ca. 1640, 1480, and 1240 cm^{-1} on Pt/Al_2O_3. The results were in agreement with the frequencies of bicarbonate which were measured on Al_2O_3 by Amenomiya et al. [19]. On the other hand, bands were observed at ca. 1550, 1300, and 1060 cm^{-1} on Pt/ZrO_2. As those were in accordance with observation on ZrO_2 by Kondo et al. [20], the species would be assigned to bidentate carbonate.

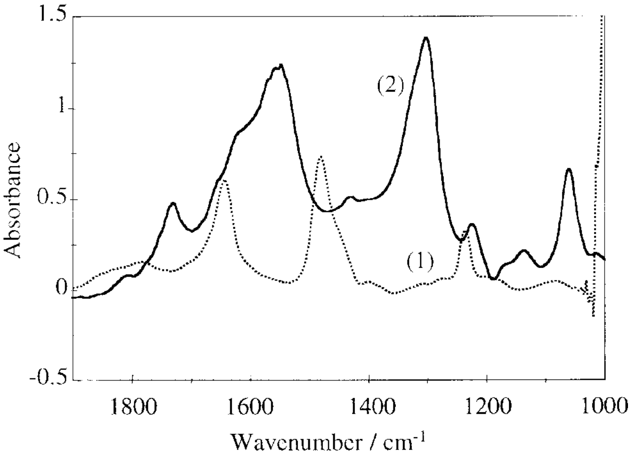

Figure 8. IR spectra of CO_2 adsorption on (1) Pt/Al_2O_3 and (2) Pt/ZrO_2 catalysts at 300 K.

4. Discussion

4.1. Reactivity and composition of deposited coke

Our earlier work has revealed the methane-derived coke (CH_x) on Pt particles can be reacted with CO_2 at 1070 K, and imbalance of CH_4 dissociation and its removal by CO_2 causes the coke. Further, we have proved that the nature of the coke on the supported Pt catalysts after exposure to CH_4/CO_2 is similar to that after exposure to CH_4/He, and coke hardly deposits on Pt/ZrO_2 after exposure to CH_4/CO_2 [16]. Hence, the nature of the coke is investigated after the catalyst is exposed to CH_4/He in this paper.

Though the amount of coke deposition increased with time of exposure to CH_4/He (from 10 to 60 min) (figures 4 and 5), the size of the TPH peak of CH_4 decreased for both catalysts (figure 2) (note that coke removal began at the same temperatures for different exposure time), implying some of the coke transformed to a less reactive form and the peak top shifted to high temperature. This result indicates that coke reactivity with H_2 highly depends on the quality of coke. Indeed, TPH has been used to investigate the nature and reactivity of the carbon on the catalyst and the peak appearance temperature is related to the composition of the carbon [21–23]. Erdőhelyi et al. [23] distinguished three forms of carbon on Rh supported catalysts: (i) the highly reactive carbidic form, which can be hydrogenated even below 350–400 K, (ii) a less reactive amorphous layer, $T_p = 235$–495 K, and (iii) the relatively inactive graphitic form, which reacts with hydrogen only above 650 K. In our experiments, the coke on Pt/Al_2O_3 and Pt/ZrO_2 was barely activated to CH_4 above 873 and 1073 K, respectively (figure 2), and some of the coke could not be removed by H_2 even at 1273 K. From the above consideration, the form of coke on Pt/Al_2O_3 and Pt/ZrO_2 would be graphitic. Further, coke reactivity with H_2 was higher on Pt/Al_2O_3 than on Pt/ZrO_2, indicating the reactivity of coke itself on Pt/Al_2O_3 would be higher than that on Pt/ZrO_2. The difference of coke reactivity between Pt/Al_2O_3 and Pt/ZrO_2 could be attributed to the difference of its crystallinity. The crystallinity of coke would be higher on Pt/ZrO_2 than on Pt/Al_2O_3.

4.2. Relevance of the coke (on Pt) reactivity with H_2, O_2, and CO_2 between Pt/Al_2O_3 and Pt/ZrO_2

As we have investigated the reactivity of coke (on Pt) with H_2 (figures 1–3), O_2 (figures 4 and 5), and CO_2 (figure 6) after Pt/Al_2O_3 and Pt/ZrO_2 were exposed to CH_4/He, we summarize here the factors affecting the peak appearance temperature.

During TPH coke activation would mainly depend on the reactivity of coke. On the other hand, during TPO and TPRn with CO_2 it could depend on coke reactivity and/or reactivity of O_2 and CO_2. O_2 activation ($O_2 \rightarrow 2O$) and CO_2 activation ($CO_2 \rightarrow CO + O$) would be catalyzed on the active site which is related with the oxide support, for example, by presence of an oxygen lattice defect on support [24], and through the formation of carbonate on support in the case of CO_2 [13–15]. Our results (figures 2–6) showed the reactivity of coke with H_2 is lower on Pt/ZrO_2 than on Pt/Al_2O_3, and, in contrast, the reactivity of coke with O_2 and CO_2 (corresponding to lower temperature peak on Pt/ZrO_2, which was related to catalyst stability) on Pt/ZrO_2 is higher than that on Pt/Al_2O_3. The reactivity of coke with H_2 would be mainly affected by the coke reactivity itself, and, on the other hand, the reactivity of coke with O_2 and CO_2 (for Pt/ZrO_2, lower temperature peak) would be more strongly affected by O_2 and CO_2 activation. During CH_4/CO_2 reforming reaction coke would be removed by reaction with CO_2; this process would highly depend on the activation of CO_2, i.e., depending on the nature of support.

4.3. Comparison of the CO_2 activation between Pt/ZrO_2 and Pt/Al_2O_3

In earlier works, CO_2 activation has been related to carbonate type species on supports [13–15], and bicarbonate and bidentate type carbonate were detected on Pt/Al_2O_3 and Pt/ZrO_2, respectively, in this communication. If the CO_2 activation occurs via those species, as implied in the earlier studies [13–15], the current IR results may imply that formation of bidentate carbonate leads to easier activation of CO_2 than via formation of bicarbonate.

Then, we study here the CO_2 activation on the oxygen defect sites. The results of CO evolution measurement during CO_2 flow revealed that the ability of CO_2 activation (= producing active oxygen: $CO_2 \rightarrow CO + O$) is higher on Pt/ZrO_2 than Pt/Al_2O_3 (tables 1 and 2). The difference would be attributed to the reducibility of Zr^{4+} (to Zr^{n+}) for producing oxygen defect sites. Under CH_4/CO_2 condition, coke would react with the active oxygen (produced on the oxygen defect sites) to produce CO, and the oxygen defect sites would be replenished by CO_2 (cycled) [24].

5. Conclusions

The stability of supported Pt catalysts for CH_4/CO_2 reforming depends crucially on the support. Pt/ZrO_2 has stable activity, while Pt/Al_2O_3 deactivated slowly with time on stream. The cause of deactivation on Pt/Al_2O_3 was attributed to coke deposition on Pt. On the other hand, coke hardly deposits on Pt/ZrO_2. One of the factors causing the high coke resistance of Pt/ZrO_2 was attributed to higher coke reactivity with CO_2 on Pt/ZrO_2 than on Pt/Al_2O_3 [16].

The reactivity of coke itself (on Pt) was higher on Pt/Al_2O_3 than on Pt/ZrO_2. However, the coke reactivity with CO_2 was inverse. The different coke reactivity with CO_2 is not attributed to the distinction of coke reactivity. The ability of CO_2 activation on the active site (probably oxygen defect site of the support) would be higher on Pt/ZrO_2 than on Pt/Al_2O_3. Therefore, the high reactivity of coke towards CO_2 on Pt/ZrO_2 was attributed not to the reactivity of coke itself, but to the high ability for CO_2 activation.

References

[1] K. Seshan, J.H. Bitter and J.A. Lercher, Chem. Tech., in press.
[2] J.T. Richardson and S.A. Paripatyadar, Appl. Catal. 61 (1990) 293.
[3] S.T. Ashcroft, A.K. Cheetham, M.L.H. Green and P.D.F. Vernon, Nature 352 (1991) 225.
[4] N.R. Udengaard, J.-H. Bak Hansen, D.C. Hanson and J.A. Stal, Oil Gas J. 90 (1992) 62.
[5] J.R. Rostrup-Nielsen and J.-H. Bak Hansen, J. Catal. 144 (1993) 38.
[6] J.R. Rostrup-Nielsen, Catal. Today 18 (1993) 305.
[7] V.A. Tsipouriari, A.M. Estathiou, Z.L. Zhang and X.E. Verykios, Catal. Today 21 (1994) 579.
[8] K. Seshan, H.W. ten Barge, W. Hally, A.N.J. van Keulen and J.R.H. Ross, Stud. Surf. Sci. Catal. 81 (1994) 285.
[9] H.M. Swaan, V.C.H. Kroll, G.A. Martin and C. Mirodatos, Catal. Today 21 (1994) 571.
[10] K. Seshan, P.D.L. Mercera, E. Xue and J.R.H. Ross, US Patent 537791 (1994); Japan Patent 522634 (1994); International Patent WO 94/224042 (1994).
[11] Z. Zhang, X.E. Verykios, S.M. MacDonald and S. Affrossman, J. Phys. Chem. 100 (1996) 744.
[12] K. Tomishige, Y.-G. Chen and K. Fujimoto, J. Catal. 181 (1999) 91.
[13] J.H. Bitter, K. Seshan and J.A. Lercher, J. Catal. 171 (1997) 279.
[14] J.H. Bitter, K. Seshan and J.A. Lercher, J. Catal. 176 (1998) 93.
[15] J.H. Bitter, K. Seshan and J.A. Lercher, J. Catal. 183 (1999) 336.
[16] K. Nagaoka, K. Seshan, K. Aika and J.A. Lercher, J. Catal., submitted.

[17] J.H. Bitter, K. Seshan and J.A. Lercher, Topics Catal. 10 (2000) 295.

[18] K. Foger, in: *Catalysis – Science and Technology*, Vol. 6, eds. J.R. Anderson and M. Boudart (Springer, Berlin, 1974).

[19] Y. Amenomiya, Y. Morikawa and G. Pleizier, J. Catal. 46 (1977) 431.

[20] J. Kondo, H. Abe, Y. Sakata, K. Maruya, K. Domen and T. Onishi, J. Chem. Phys. 84 (1988) 511.

[21] F. Solymosi, A. Erdőhelyi and J. Cserényi, Catal. Lett. 16 (1992) 399.

[22] T. Koerts, M.J.A.G. Deelen and R.A. van Santen, J. Catal. 138 (1992) 101.

[23] A. Erdőhelyi, J. Cserényi and F. Solymosi, J. Catal. 141 (1993) 287.

[24] A.M. O'Connor, F.C. Meunier and J.R.H. Ross, Stud. Surf. Sci. Catal. 119 (1998) 819.